JPL D-3722
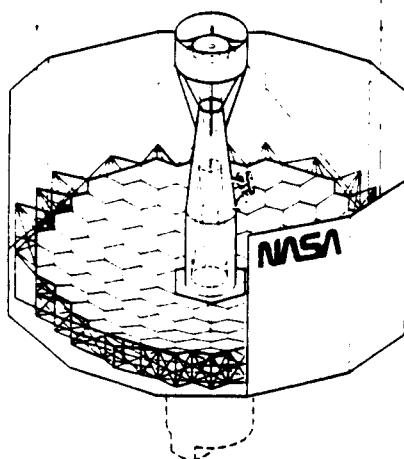
LDR Technical Memorandum 86-2

Wavefront Error Sensing

Dr. Eldred F. Tubbs

October 15, 1986

National Aeronautics and
Space Administration

JPL

Jet Propulsion Laboratory
California Institute of Technology
Pasadena, California

15 Pgs. (Inc. title pg.)

WAVEFRONT ERROR SENSING FOR LDR
Eldred F. Tubbs

Wavefront sensing is a significant aspect of the LDR control problem and requires attention at an early stage of the control-system definition and design. This memo reports a first step in the direction of defining wavefront-sensing requirements and approach by selecting two specific, proven techniques and formulating a wavefront-sensing approach for LDR. It is not the purpose to select a recommended approach. That would be premature as further study will yield other approaches based on other sensing techniques. Rather, the purpose is to improve the definition of the wavefront-sensing subsystem, to identify the requirements that this subsystem imposes on LDR configuration and operations, and to determine particular areas for more detailed study.

The Problem. If LDR is to achieve the required performance it will be necessary to have active control of the optical configuration during the observation periods. Since the astronomical objects observed by LDR may be extended or very faint it will be difficult to use the wavefront from the object under observation to provide input to the wavefront-deformation control system, and a more complex approach must be used.

The Approach. One approach is to use an operational sequence in which the telescope is first pointed at a bright, point-like astronomical object and the optical configuration adjusted to optimize the image. Configuration sensors are then used to determine the position and orientation of the

optical elements in the system. During subsequent observation periods when the wavefront sensor cannot be used the configuration sensors monitor the system. If an optical element drifts out of position as determined by the configuration sensor the control system takes corrective action. This action can either be one which restores the wayward element to its correct position or moves some other element to compensate for the displaced one. If the latter is done, the software model of the system is used to calculate the compensation displacement, and the control problem falls into the class characterized by noncollocated sensors and actuators.

Wavefront Sensing. The approach outlined above requires two classes of sensors: wavefront and configuration. This discussion is limited to the wavefront sensing problem. A significant aspect of the problem is that of providing sufficient sensitivity at small departures from optimum wavefront and at the same time providing sensing over a sufficiently large range of wavefront errors to permit initial adjustment.

There are many approaches to wavefront measurement. It has long been a tool of the optical fabrication shop[1]. In recent years it has been of interest for the adaptive-optics problem[2], and an SPIE conference in San Diego in 1982 was devoted to it[3]. The particular approach used in this study is based on work done at Hughes on wavefront sensing and configuration adjustment and reported at that conference[4]. This work demonstrated a two-step approach in which a coarse sensor and an algorithm known as OYSTER (Optimal Yardstick Towards Error Reduction) is first used to bring the system into approximate adjustment and is followed by the EEOD (Error

Estimation from Operational Detectors) algorithm which used the output of the operational detectors to optimize the image.

The OYSTER approach is to measure wavefront slope using a Hartmann test (described below) and to calculate the required changes in the physical alignment of the system to reduce the slope errors to zero. OYSTER was demonstrated at Hughes using a 7-element reflective system with 19 degrees of freedom and a 5-aperture Hartmann mask. Each aperture of the mask produces a spot near the focal plane. The coordinates of these spots are measured, and from them the adjustments of the alignment variables are calculated using a linear approximation derived from the software model of the system. In the particular experiment a single pass through the OYSTER algorithm was sufficient to give diffraction-limited performance at 20 μm.

The EEOD approach assumes that the system has a two-dimensional array detector in the focal plane with sufficient resolution to obtain a good measure of the point-spread function (PSF). It also assumes that there is a point source in the field of view to provide a test wavefront and that the system is sufficiently well aligned to provide a reasonable PSF as a starting point. The intensity in the focal plane is a function of the coordinates in the focal plane. For a given point the intensity depends on the tilts and decenters of the elements of the system. In the algorithm, this function is represented by the first two terms of a Taylor's series. The ideal PSF is calculated from the software model of the system in a manner similar to what was done in the LDR Pathfinder Study[5] as are the

derivatives. (For laboratory-sized systems the PSF and the derivatives may be measured.)

The operation of the EEOD algorithm was also demonstrated in the laboratory using an optical system with 14 degrees of freedom. The system was an autocollimating combination of a 12-inch afocal Cassegrain and an off-axis paraboloid. The experiment was automated using motorized micrometers. The PSF was measured using a 100 x 100 pixel CCD detector.

Since EEOD requires good initial alignment, OYSTER was used first with a four-aperture Hartmann mask. This was done in two steps: a lower sensitivity one for initial alignment and a higher sensitivity one with 10 times magnification for the final adjustment. In the particular experiment it was possible to produce diffraction-limited performance using only the OYSTER system. Accordingly, it was necessary to introduce errors into the PSF by making random adjustments of actuators. It was found that tilt and defocus of the secondary mirror could be corrected in one iteration. When decenter was added, two iterations were required.

Application to LDR. The optical layout of LDR and segment pattern of the primary are shown in Figure 1 while the refractive equivalent is shown in Figure 2. In Figure 2, the solid lines show the imaging of an astronomical object on the focal plane and the dashed lines show the imaging of the primary on the quaternary.

The OYSTER algorithm uses a Hartmann test to measure the wavefront. This is
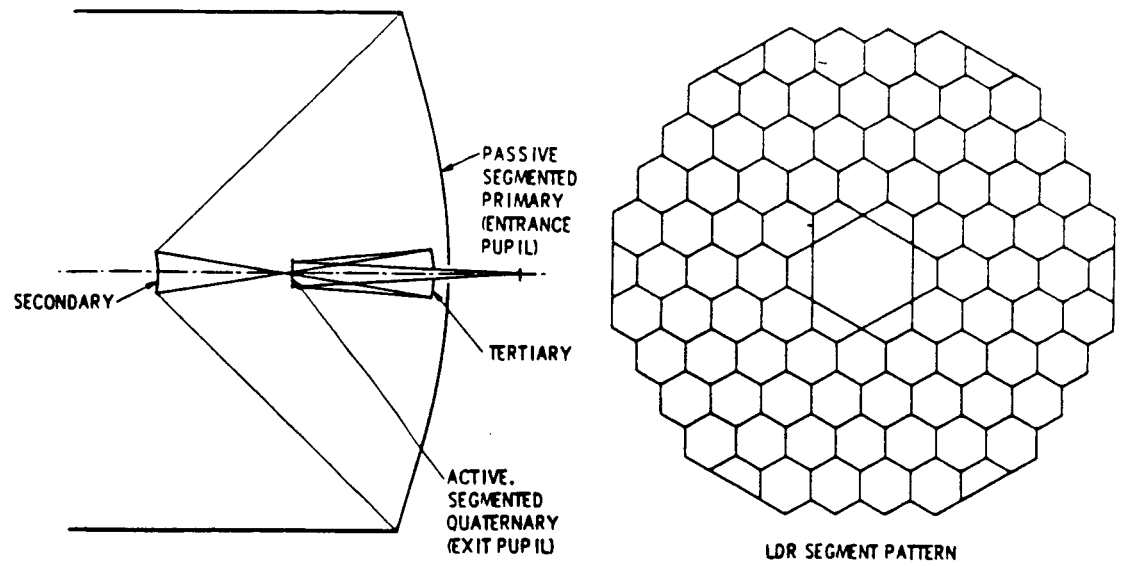
4

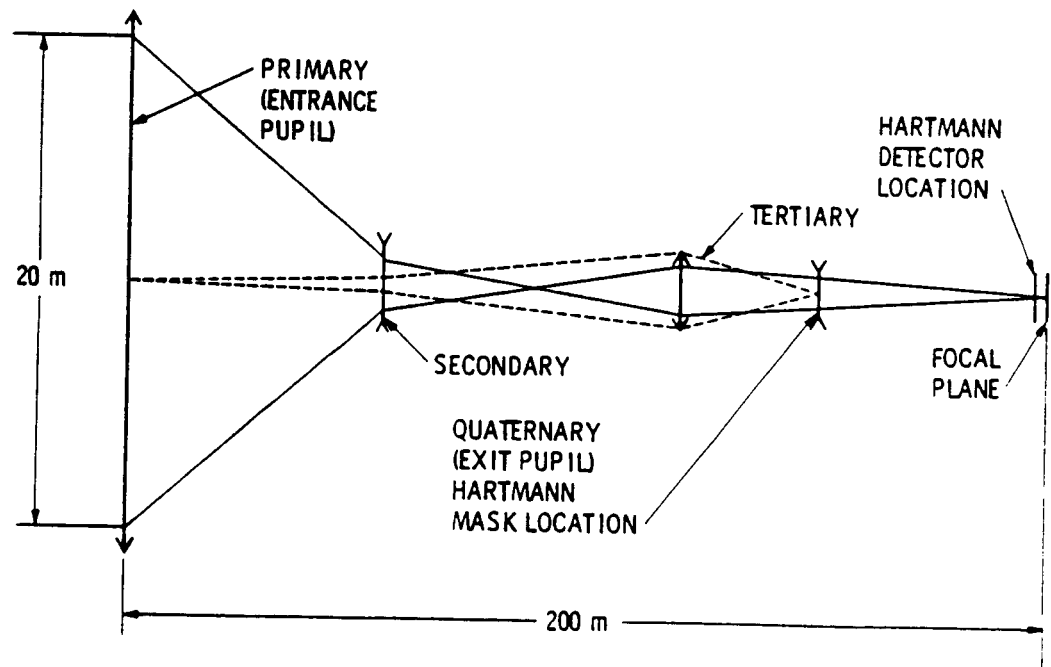FIGURE 1. OPTICAL LAYOUT OF LDR

FIGURE 2. REFRACTIVE EQUIVALENT OF LDR

a geometrical test and does not require the system to be near diffraction-limited performance. The elements of a Hartmann test as applied to a system like LDR are:

1. A test wavefront. For telescopes this is generally from a distant point source such as a star.

2. A diaphram or mask pierced with multiple apertures which divide the incoming wavefront into separate beams.

3. An array detector near the focal plane which can intercept the beams on a reference surface.

The individual beams define the normal to the wavefront and their intercept on the reference surface can be calculated from the software model of the system. Comparison of the calculated and measured intercepts gives a measure of the slope error of that portion of the wavefront.

The two-stage[6] configuration of LDR faciliates the use of a Hartmann test. The mask is located at the quarternary. It must be deployable, but this can be accomplished by making it segmented as shown in Figure 3. The 12 segments can be hinged along their outer edges. The configuration shown is for a 90 segment mirror and has one aperture per segment. The apertures shown in the figure are approximately 40 mm in diameter. The mask itself is approximately one meter across.
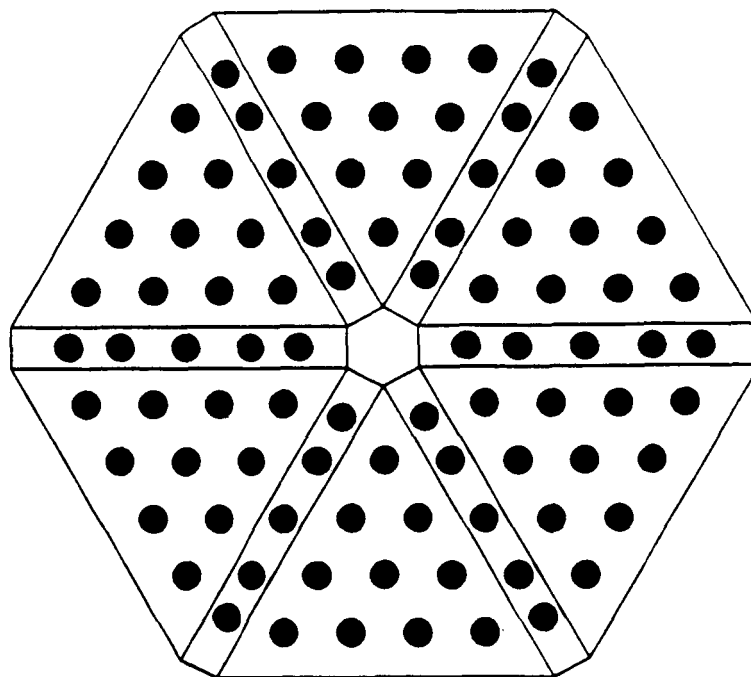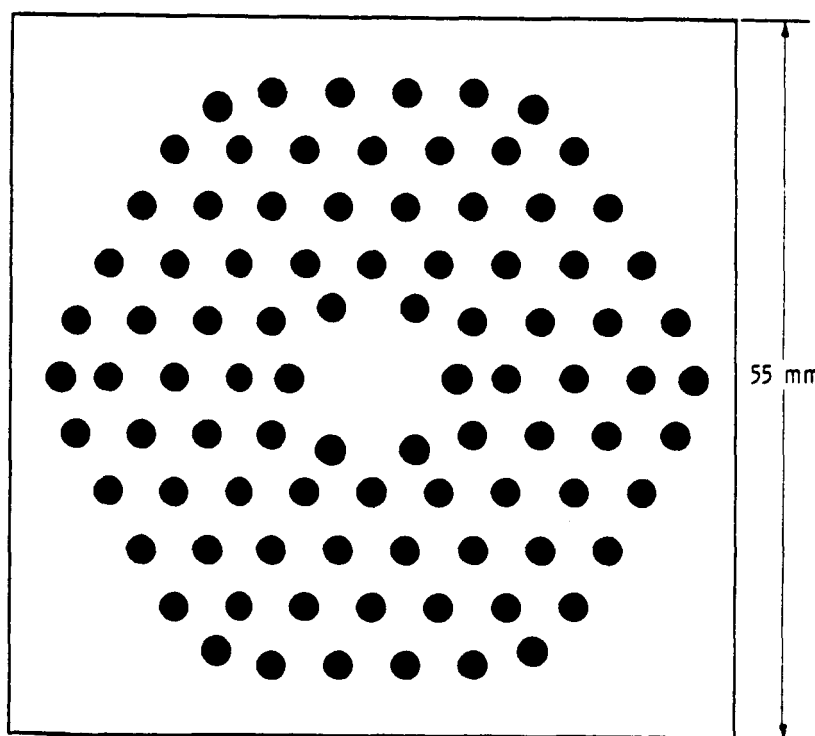
FIGURE 3. HARTMANN MASK FOR LDR

FIGURE 4. SPOT PATTERN ON DETECTOR

The ease with which a Hartmann test can be applied to LDR depends on the wavelength range of the system. If the reflectivity, surface finish, and figure of the optics allow operation at relatively short wavelength, the situation is quite straightforward. This is illustrated in Figure 4, which shows a Hartmann pattern for a 90 segment mirror observed approximately one-half meter in front of the focal plane using the mask of Figure 3. The spot size shown in Figure 4 is determined by geometrical considerations only and does not show diffraction spreading. At 1 μm the diffraction will result in a 25% increase in diameter on the spots. At 5 μm wavelength will approximately double their size and probably represents an upper limit on the wavelength that can be used for a Hartmann test.

The outline around pattern in Figure 4 indicates the size of a large CCD detector currently offered by Tektronix. Spots of the size shown spread over many pixels on the detector and result in accurate centroid. The question of the availability of astronomical objects suitable as sources has not been investigated. A rough estimate based on the experience with the ASTROS star tracker is that a few seconds integration time would give sufficient signal at a wavelength of 1 μm. The situation for longer wavelengths must be investigated.

The conclusion from this consideration is that the Hartmann test and hence and algorithm similar to OYSTER can be used for the initial alignment of LDR provided quality of the optics allows operation at wavelengths shorter than 5 μm, an array detector of sufficient size, resolution, and sensitivity is available for this wavelength, and there are a sufficient number of point-

like astronomical sources with sufficient flux at this wavelength.

Since there are 90 Hartmann spots, there will be 180 coordinates as input to the algorithm. If the axis of the average paraboloid through the surface of the primary is taken as a reference direction, there will be two degrees of freedom locating this direction with respect to the source. The symmetry of the secondary and tertiary results in five degrees of freedom for each. The quarternary will have six since its segments must be registered with those of the primary and the individual segments will each have three degrees of freedom. For the 90-segment system, the total number of degrees of freedom is 288. The matrix is 180 x 288, but many of the elements will be zero. The computational question requires further study.

The application of EEOD to LDR poses a somewhat different problem. The radius of the Airy disk is approximately 0.6 mm at 50 μm. the shortest wavelength assumed for diffraction-limited performance, and is proportionally larger for longer wavelengths. Since the EEOD concept calls for measuring the point-spread function with the science detectors, the way in which it is done is dependent on the final choice for those detectors.

Once these detectors have been chosen, the approach to PSF measurement can be addressed in more detail. Some of the considerations are addressed below to the extent that they can be at this time.

As with the Hartmann test, the question of the availability of point-like sources is important. At longer wavelengths there are non-thermal point sources. At shorter wavelengths thermal sources are strong enough. The

diffraction-limited region of LDR falls between these regions and the question of availability of sources which are sufficiently bright, sufficiently point like, and sufficiently numerous must be answered.

If LDR is provided with an array detector of sufficient resolution in the diffraction-limited region, the point-spread function can be measured using it. In addition to the basic resolution of the detector, the pointing jitter and required signal-integration time will limit the accuracy with which the PSF can be determined. The jitter specification is for less than 0.02 arc sec over three minutes. That is approximately 1/60 of the Airy disk diameter at the shortest diffraction-limited wavelength and would appear to be sufficiently small for wavefront determination.

If array detectors are not available for wavelengths within the diffraction-limited region, it will be necessary to determine the PSF by scanning. This could probably be done best with a scanning mirror near the focal plane. At a minimum, the scanned area should be three times the Airy-disk diameter with a minimum of 100 pixels per side. If the scanning is to be completed within the specified interval for stable pointing of three minutes, the rate will have to be approximately 60 pixels per second. This must be compared with projected detector performance as it becomes available.

Finally, detailed calculations must be made using the optical model to determine the degree of sensitivity that can be achieved with the EEOD algorithm. In the Hartmann test there is a spot for each segment. If a segment is not correctly oriented, the corresponding spot is out of position

and the error is easily identified and corrected. The Hartmann test is not sensitive to piston errors and these must be detected from the PSF. When the number of segments is small, the PSF is quite sensitive to piston displacements. This was shown in the work with a seven-segment reflector in the Pathfinder Study[5]. It was shown there that a $\lambda/7$ piston displacement of one segment dropped the peak intensity of the PSF to 78% of the ideal. With 90 segments the sensitivity to the displacement of an individual panel will be much less and may be undetectable. However, the plan for constructing the primary support structure calls for attaching adjoining panels to common supports. If these attachments can be made with high precision, piston displacement of a single panel will not be possible. This is a significant issue and the question of detecting piston displacement of panels can only be answered by detailed modeling of the optical system and mechanical system.

Summary. A two-step approach to wavefront sensing for LDR has been examined. A Hartmann test for coarse alignment, particularly segment tilt, seems feasible if LDR can operate at 5 μm or less. The direct measurement of the point-spread function in the diffraction-limited region may be a way to determine piston error, but this can only be answered by a detailed software model of the optical system. The question of suitable astronomical sources for either test must also be addressed.

References

1. Optical Shop Testing, Daniel Malacara, Ed., John Wiley and Sons, New York, 1978.

2. Journal of the Optical Society of America, 67, No. 3 (1977)

3. Proc. SPIE No. 351, Wavefront Sensing (1982)

4. N. Wu, B. L. Ellerbroek, S. G. Williams, Experimental Verification of an Image-Based Alignment Technique for Optical Systems in Space. Proc. SPIE 351, 121 (1982)

5. P. N. Swanson and G. W. Null, Large Deployable Reflector-Pathfinder Study Report, JPL P-195 (December 1982) pp. 6-67 to 6-73.

6. P. N. Swanson, et. al., System Concept for a Moderate Cost Large Deployable Reflector (LDR), Optical Engineering 25, 1045, (1986)
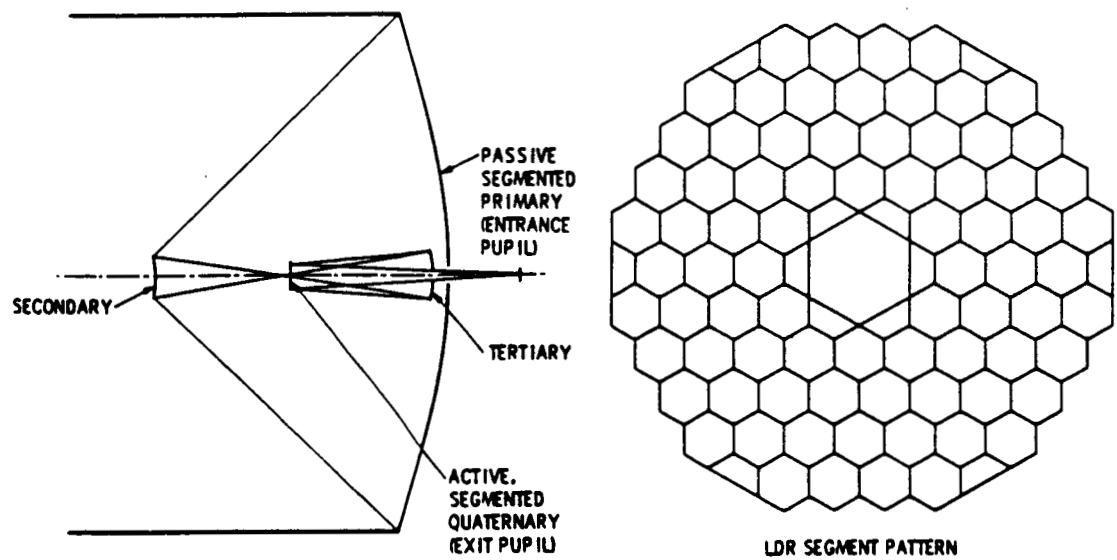
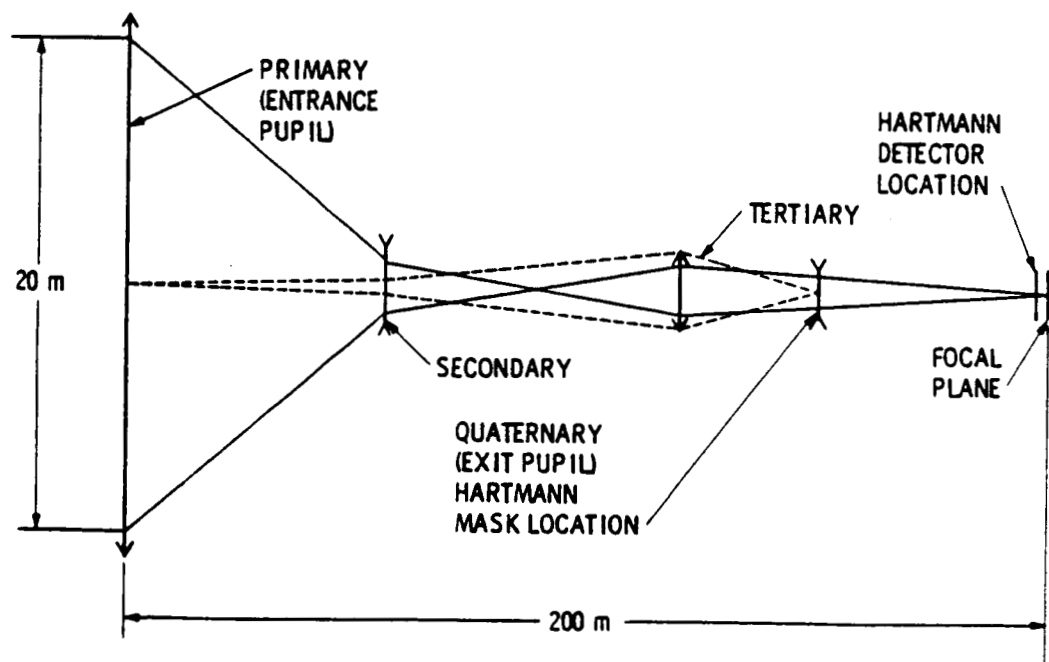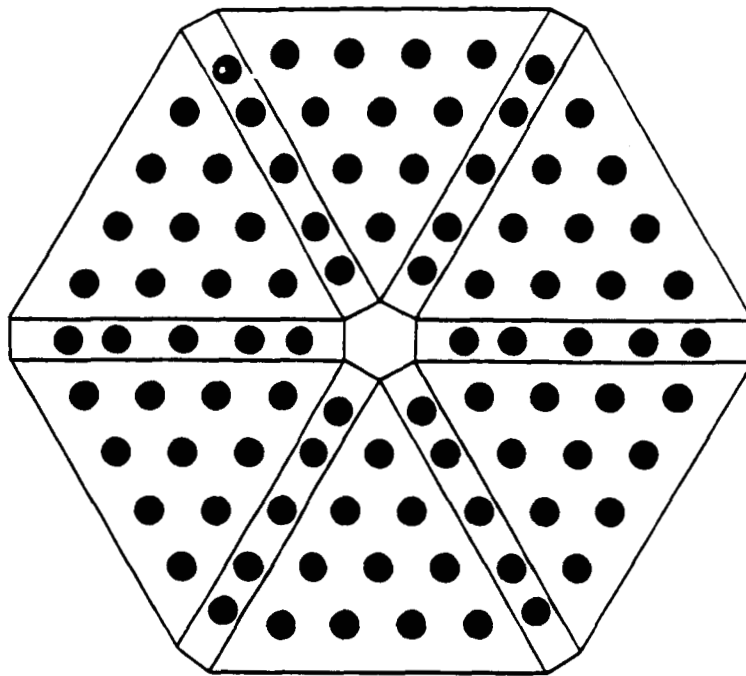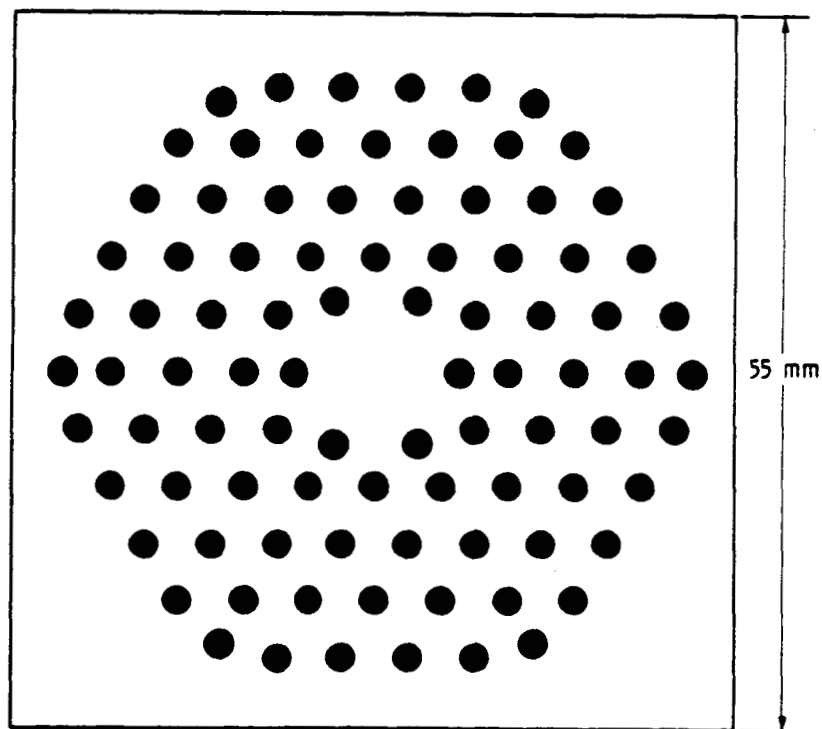FIGURE 1. OPTICAL LAYOUT OF LDR

FIGURE 2. REFRACTIVE EQUIVALENT OF LDR

FIGURE 3. HARTMANN MASK FOR LDR

FIGURE 4. SPOT PATTERN ON DETECTOR